

Demonstration of strong coupling of a subradiant atom array to a cavity vacuum

B. Gábor,^{1,2} K. V. Adwaith,^{1,3} D. Varga,^{1,4} B. Sárközi,¹ A. Dombi,¹ T. W. Clark,¹ F. I. B. Williams,¹ D. Nagy,^{1,*} A. Vukics,¹ and P. Domokos¹

¹*HUN-REN Wigner RCP, H-1525 Budapest P.O. Box 49, Hungary*

²*Department of Theoretical Physics, University of Szeged, Tisza Lajos körút 84, H-6720 Szeged, Hungary*

³*Université Paris-Saclay, CNRS, ENS Paris-Saclay, CentraleSupélec, LuMin, 91190 Gif-sur-Yvette, France*

⁴*Department of Physics of Complex Systems, ELTE Eötvös Loránd University, Pázmány Péter sétány 1/A, H-1117 Budapest, Hungary*

(Dated: October 2, 2024)

By considering linear scattering of cold atoms inside an undriven high-finesse optical resonator, we experimentally demonstrate effects unique to a strongly coupled vacuum field. Arranging the atoms in an incommensurate lattice, with respect to the resonator mode, the scattering can be suppressed by destructive interference: resulting in a subradiant atomic array. We show however, that strong coupling leads to a drastic modification of the excitation spectrum, as evidenced by well-resolved vacuum Rabi splitting in the intensity of the fluctuations. Furthermore, we demonstrate a significant polarization rotation in the linear scattering off the subradiant array via Raman scattering induced by the strongly coupled vacuum field.

I. INTRODUCTION

Atoms can often be treated as linearly polarizable particles when weak illumination keeps them in the low-saturation regime. Even when the complicated internal electronic structure does not play any role, the interaction with low-intensity light, basically Rayleigh scattering, can still produce a wealth of interesting phenomena, depending on the specific electromagnetic configuration. Collective atomic emission, for example, is of great interest, particularly in the context of superradiance [1–5] and subradiance [6–8]. The latter has application in long-term storage of quantum information [9–11]. Accordingly, there has been an extensive study of regular three-dimensional atomic arrays [12] in which there is destructive interference of the scattered light by geometric constraints. Increased storage time, i.e., the collective inhibition of spontaneous emission has been shown to correspond to optical guided modes in the atomic array [13]. Beyond ordering atoms, the radiation can also be shaped to favour scattering into selected output channels, such as when coupling to fibre-guided modes, [14, 15] where subradiant configurations have been both predicted and experimentally demonstrated [16].

In this paper, we revisit low-intensity light scattering from a one-dimensional subradiant array, when the scattered output is directed into strongly coupled radiation modes sustained by an optical resonator [17, 18]. Dynamics of laser-driven atoms interacting with cavity field modes is of high interest producing a great variety of effects: experiments started with efficient cooling schemes [19], atomic self-organization [20–22] and led to the exploration of superradiant [23–25] and other types of quantum phase transitions [26–36]. Collective radia-

tion effects in many-atom cavity QED systems have been explored, such as the interference in Rayleigh scattering with controlled positioning of atoms in a cavity mode [17, 18, 37–39], quantum non-demolition measurements [40], as well as lasing [41, 42] and superradiant lasing [43–45] with cold atoms as the gain media.

We will explore the spectral and polarization properties of scattering from a cold atomic ensemble into a quasi-resonant mode of a high-finesse optical cavity. As it was discussed in [13], subradiance is linked to a polariton mode of the many-body system. Accordingly, in the cavity context, we will give experimental evidence that the destructive interference in a subradiant configuration of scatterers does not amount to a decoupling from the cavity field. Although no coherent field builds up in the cavity, a strong collective coupling between the atomic ensemble and a cavity mode is manifested by vacuum Rabi splitting [46–48] in the spectrum of the outcoupled cavity field intensity fluctuations. We reveal another remarkable effect, i.e., the rotation of field polarization by the subradiant array. In coherent scattering, the dipole oscillation of an atom is parallel with the polarization of the impinging field; hence, the scattered field preserves this polarization. This component is, however, suppressed by the destructive interference. The incoherent scattering is enhanced in a high-finesse cavity also into the mode with polarization orthogonal to that of the incoming field. The polarization rotation is accompanied by a two-photon Raman transition in the atomic hyperfine ground state manifold in accordance with the conservation of angular momentum [24, 49, 50]. We show that this process is on the same order of the drive power and reflects the same vacuum Rabi split spectrum as the polarization-preserving scattering.

* Corresponding author:nagy.david@wigner.hun-ren.hu

II. RESULTS

The experimental scheme is sketched in Fig. 1. Ru-

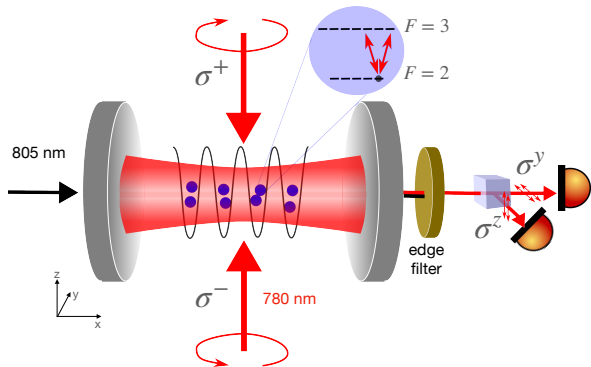


FIG. 1. Scheme of our experiment on the scattering from a subradiant atomic configuration. Cold ^{87}Rb atoms in an intra-cavity dipole lattice at wavelength 805 nm are illuminated by two counter-propagating coherent laser beams with equal intensity and opposite circular polarizations from the two opposite directions perpendicular to the cavity axis. The laser was set near resonant with the $F = 2 \leftrightarrow F = 3$ transition of the D2 line at 780 nm and close to resonance with one of the fundamental cavity modes. The cavity field output is monitored by single photon counters on discriminating the photon polarization. The cavity linewidth is $\kappa = 2\pi \times 3$ MHz (HWHM), the maximum single-atom coupling constant is $g = 2\pi \times 0.33$ MHz.

bidium atoms were collected in an 805 nm optical lattice, using a longitudinal mode of a high-finesse linear cavity and so captured far from any natural atomic resonance [51]. The atomic cloud was then transversely pumped at an angular frequency ω , with varying detuning from the $F = 2 \leftrightarrow F' = 3$ transition, ω_A . The angular frequency ω_C of another (undriven) longitudinal mode was set to resonance with ω_A , such that the transverse drive had equal detuning with respect to the atom, $\Delta_A \equiv \omega - \omega_A$, as it had to the cavity mode, $\Delta_C \equiv \omega - \omega_C$, i.e. $\Delta \equiv \Delta_A = \Delta_C$. Cavity photons could be generated only by scattering from the laser drive beams. Since the atomic distribution had a periodicity incommensurate with the wavelength of the drive (780 nm), the scattered wave components from different positions of the mode were expected to have averaged out along the cavity axis [18, 52]. Such destructive interference is imposed by the geometry, regardless of the intensity, detuning and polarization of the drive. Even if coherent field build-up in the cavity mode was suppressed, we expected that photon field fluctuations would be present. Such was the case, and we recorded the field outcoupled from the cavity by single photon counters, discriminating their polarization linearly, i.e. along ‘y’ and ‘z’ in Fig. 1.

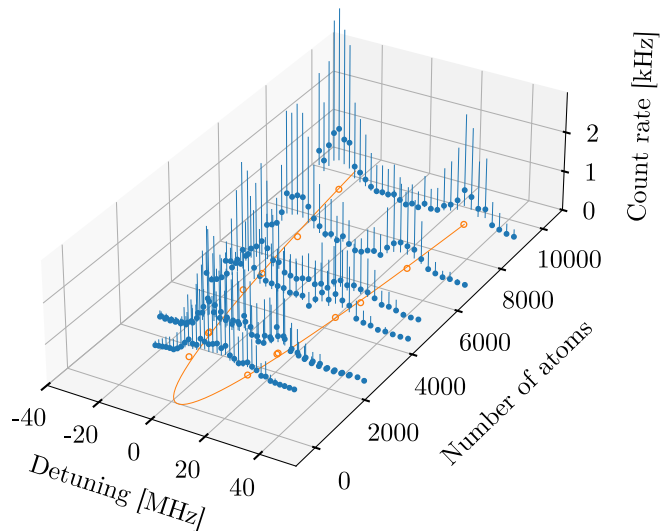


FIG. 2. Vacuum Rabi splitting with a subradiant array of atoms. The photon count rate in the first 1 ms of exposure time is plotted versus the laser drive detuning Δ for various atom numbers N . Each point and error bar is obtained from an ensemble of 70 runs assuming log-normal distribution, given that the photon count rate is a priori a non-negative quantity. The maxima of the doublets, projected on the bottom plane (green circles), fit well on a parabola $N = \Delta^2/g_{\text{eff}}^2$ with $g_{\text{eff}} = 2\pi \times 0.26$ MHz, in accordance with the \sqrt{N} dependence known for the collective coupling of a number of N atoms to a single cavity mode.

A. Vacuum Rabi splitting

As a first step, the number of atoms loaded into the mode volume was varied in the range of ~ 1500 to $\sim 10^4$ by setting different MOT cycle protocols. The effective atom number was determined from independent measurements: it was calibrated by the cavity transmission of a near resonant probe detuned from the atomic transition such that the atoms acted as a dispersive medium. The drive laser intensity was lowered as much as possible so that a reasonable rate of photons, scattered by the atoms into the cavity and then outcoupled from it, could be detected by the single photon counters. At fixed atom number and drive intensity, the drive laser detuning Δ was varied in the range of ± 50 MHz to record a spectrum. Figure 2 presents that the intensity fluctuations reflected the vacuum Rabi splitting for large enough atom number. The observed large variance is intrinsic to the photon statistics: it indicates that the mean-field vanishes, which is in agreement with our expectation that the atoms ordered with a periodicity of the half of the 805 nm wavelength form a subradiant configuration. This expectation was verified in a subsequent step by a more involved analysis. The spectra have been fit by a sum of two Lorentzians providing for the peak maxima indicated by empty green circles in the bottom plane. The parabola fit on these peak positions is thus a \sqrt{N} function, clearly

evidencing that a strong collective coupling between the atomic ensemble and the mode is present. The coefficient $g_{\text{eff}} \approx 2\pi \times 0.26$ MHz from the fit is in good agreement with the expected value of $2\pi \times 0.225$ MHz which can be obtained by averaging over the atomic population distributed evenly in the $F = 2, m_F$ magnetic sublevels with different Clebsch-Gordan coefficients. We attribute the 10% deviation to the small but not entirely negligible saturation in the atom number calibration measurement.

B. Linear scattering

In the next step, we analysed the vacuum Rabi splitting spectrum for a range of drive powers in order to verify that the scattering is in the linear regime. The recorded spectra could be compared to a simple theory based on a linear polarizability model of atoms [53] which assumes that the atomic induced dipole is proportional to the local electric field, $\vec{d} \propto \epsilon_0 \chi(\omega) \vec{E}(\vec{r})$ in the low-excitation limit [54].

In our configuration, the two counterpropagating beams have opposite circular polarizations. The resulting electric field is linearly polarized in a helical pattern along the drive axis ‘z’, i.e., $\vec{E}(\vec{r}) \parallel \vec{e}_y \cos kz + \vec{e}_x \sin kz$. Note that the optical resonator does not sustain modes with \vec{e}_x polarization, being the direction of the cavity axis; hence, effectively, only the linear polarization \vec{e}_y couples into the resonator field. Linear scatterers lead then to the intracavity field amplitude for the mode polarized in the direction ‘y’ [18, 54]

$$\alpha_y = \frac{\eta g \sum_a \cos kx_a \cos kz_a}{(i\Delta_A - \gamma)(i\Delta_C - \kappa) + g^2 \sum_a \cos^2 kx_a}, \quad (1)$$

where η is an effective drive amplitude and the summation goes over the atoms indexed by $a = 1 \dots N$ with positions \vec{r}_a . The modulus square of the denominator has two minima which, for our setting of resonance between the atoms and the mode, $\Delta_A = \Delta_C = \Delta$, are at $\Delta = \pm \sqrt{g^2 \sum_a \cos^2 kx_a} \equiv \pm \sqrt{N_{\text{eff}}} g$. The effective atom number is around $N_{\text{eff}} \approx N/2$ for $\overline{\cos^2 kx} = 1/2$. This two-peaked resonance behaviour is responsible for the normal mode splitting shown in Fig. 2. A destructive interference leads to vanishing mean field, $\bar{\alpha}$, which is formally represented by that the numerator averages out to zero over the atomic positions, $\langle \sum_a \cos kx_a \cos kz_a \rangle = 0$. This is the case for a homogeneous distribution, and also for a set of positions $\{x_a\}$ sampling the 805 nm wavelength optical lattice. Even if the mean vanishes, however, there are finite size fluctuations of the atomic distribution which result in cavity field intensity fluctuations, $|\Delta\alpha_y|^2 \neq 0$. Considering the atomic positions as random variables, the statistical average gives

$$\left\langle \left| \sum_a \cos kx_a \cos kz_a \right|^2 \right\rangle \approx N^\beta / 4, \quad (2)$$

where the proportionality to the number of atoms has been taken into account with an exponent β . The actual value of the exponent can be deduced from our measured data and gives information on the atomic distribution. For destructive interference $\beta = 1$; this is expected for our case, where the distribution of atoms is incommensurate with the mode function $\cos kx$. If $\beta > 1$ was measured, it would imply the presence of a coherent component in the field amplitude, ultimately, exponent $\beta = 2$ would correspond to superradiance and perfect constructive interference. In the large vacuum Rabi splitting regime and in leading order of $(\kappa^2 + \gamma^2)/N_{\text{eff}} g^2 \ll 1$, the spectrum of the intensity fluctuations around the peak maxima can be approximated by

$$S_y(\Delta) \approx \frac{\eta^2 N^{\beta-1}}{8} \left[(\Delta \pm \sqrt{N_{\text{eff}}} g)^2 + \left(\frac{\kappa + \gamma}{2} \right)^2 \right]^{-1}. \quad (3)$$

This form of the Rabi splitting peaks can be tested experimentally to verify the linear polarizability model of atoms. Moreover, this is a crucial result because it provides a direct measure of β via the scaling of the peak intensity with the number of atoms N .

Figure 3 shows the detected photo-count rate normalized to the pump power. As shown by orange solid line, the spectrum deviates from the sum of two Lorentzian curves, in fact, the fit is composed of the sum of four Lorentzian functions. The inner two (smaller) peaks are presumably due to Raman gain similar to the effects described in [44, 49] and we will study them in a subsequent paper. The outer two resonances are in very good agreement with Eq. (3) in three features, which confirms the validity of the linear scattering regime. First, the separation of the two outer peaks, indicated by red and blue crosses in the bottom plane for the negative and positive detunings, respectively, is constant in the range of pump powers investigated. It follows then that no noticeable atomic saturation takes place. As a by-product, this peak separation can be used to calibrate N_{eff} . Second, the peak heights of the curves normalized to the input power, this latter being proportional to η^2 , are also constant, which is shown by the empty circles on the side plane. In the case of the strongest drive plotted, some tendency of shrinking peak separation and decreasing peak height can be observed, indicating that at this power the scattering begins to leave the linear regime. Third, the linewidths of the vacuum Rabi peaks, represented by the line sections in the bottom plane, are also constant and are close to the theoretical value $(\kappa + \gamma)/2$.

C. Subradiant atomic array

Having established the linearity of the scattering with driving power, we investigated the dependence of the photon fluctuations scattered into the cavity as a function of the atom number. It was changed by systematically delaying the switch-on time of the transverse drive

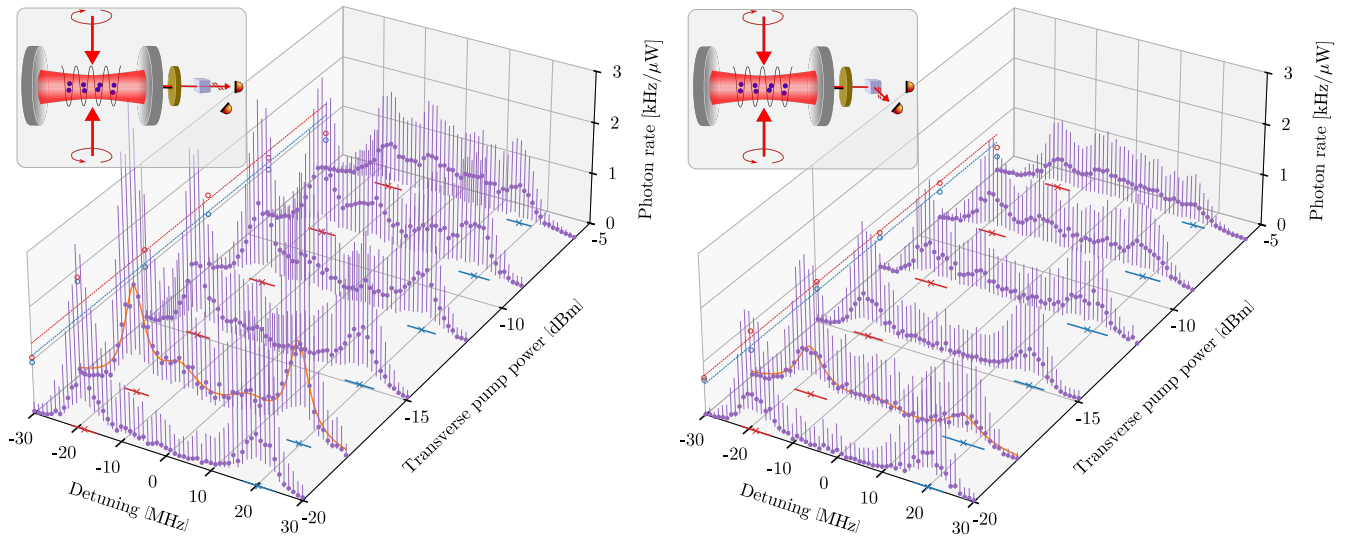


FIG. 3. Power dependence of the vacuum Rabi splitting spectrum for horizontal (a) and vertical (b) polarization. Each point is obtained from 50 runs by averaging the photon count rate in the first 100 μs of exposure. The detected photon rate is normalized to the laser drive power which was set to 10, 16, 32, 64, 128 and 256 μW for the spectra, respectively. A sum of four Lorentzian curves can be fit on each spectrum, one example is shown for the spectrum at the 16 μW drive power (orange solid line). Heights of the fit spectra are projected onto the left plane, the corresponding detunings are projected onto the bottom plane (red and blue circles and crosses for negative and positive detunings, respectively). At 256 μW , saturation effects can be noticed: the peak heights are lower, and the splitting between them is also smaller. For the drive powers being safely in the linear scattering regime, the average of their heights is shown for reference by dashed lines on the left plane, red and blue, according to the sign of detuning.

laser. The drive power was set to a low value, 16 μW (the one with the fit in Fig. 3), being clearly in the linear scattering regime. The maximum cavity photon number is estimated to be 0.014 yielding a saturation around 1.5%. The registered photo-counts were integrated over only 100 μs , in order to minimize the effects of atom loss and atomic motion. The drive frequency was tuned over the same range as in Fig. 3 so that the full spectrum was recorded. This allowed us (i) to calibrate the atom number from the distance of the peak maxima, and (ii) to determine the peak photo-count rate for the given atom number. The latter was compared with the maximum rate for vanishing detuning in the denominator of Eq. (3). The measured maximum rates, shown as a function of atom number in Fig. 4, scatter within 10% around a constant value. The experimental result is an exponent slightly below 1 which is conform with $\beta = 1$ in Eq. (3). This confirms the lack of coherent component in the scattered photon field and supports the observation of subradiance from an array of atoms. Beyond a simplified one-dimensional form of subradiance, the cavity does not merely enhance the scattering into a small solid angle for each individual atom, but the collective strong coupling to the cavity mode modifies the excitation spectrum of the atom array.

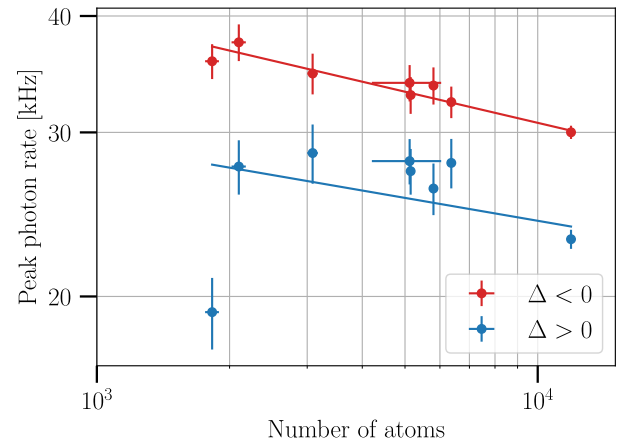


FIG. 4. Collective scattering as a function of the atom number. The maximum photon scattering rates on resonance, both at the negative (red) and positive (blue) side of the detuning, have been detected during the first time period of 100 μs time duration. Horizontal and vertical polarizations are summed up. The exponents of the linear fit on the log-log scale are obtained $\beta - 1 = -0.111 \pm 0.010$ for the red and $\beta - 1 = -0.082 \pm 0.060$ for the blue, respectively.

D. Polarization rotation

The strongly coupled vacuum field influences not only the spectral features of scattering but also the polarization, beyond the simple linear polarizability model presented above and leading to Eq. (1). The atomic polarization induced by the ‘z’ travelling σ^\pm beams is expected to excite the ‘y’ polarized mode of the cavity, which corresponds to a Rayleigh scattering process. However, in linear order of the drive intensity, we observed a photon flux emanating from the mode with polarization ‘z’ (σ_0) which is the direction of propagation of the input field. The scattering rate into the polarization ‘z’ as a function of the laser drive detuning for a range of drive powers is shown in Fig. 3(b). In full similarity with the ‘y’ polarization shown in panel (a), vacuum Rabi peaks with constant heights (normalized to the input power) and widths have been measured. The peak heights are close to those of the polarization-maintaining light scattering, which verifies that the coherent scattering from the subradiant array is strongly suppressed.

There are two sources of incoherent light: density fluctuations of Rayleigh scatterers and the incoherent scattering at the level of individual atoms. The prior can yield only ‘y’ photons; hence it underlies the difference between the recorded intensities in the two polarizations ‘y’ and ‘z’, respectively. The incoherent scattering from single atoms can be well incorporated into the semiclassical model of Eq. (1) for the cavity field amplitude α_y : the averaging over the spatial distributions along the mode function $\cos kx_a$ can be complemented by random phase factors $e^{i\phi_a}$. Such an extension does not change the spectrum and the scaling with the atom number, which was thus correctly treated for the polarization ‘y’. Concerning the polarization ‘z’, the underlying process is a Raman scattering in which the atoms undergo a hyperfine Zeeman-sublevel transition. The cavity-stimulated Raman scattering scales also linearly with the drive intensity. Note that this process has been exploited to realize quantum interfaces between light polarization and atomic memory states [55, 56] by means of stimulated adiabatic passage processes with pulsed excitation in single-atom strong-coupling cavity QED experiments. Cavity-enhanced Raman scattering has also been observed from a regular half-wavelength ordered array [18] when the drive is detuned from the atoms. In our experiment, we revealed that the Raman scattering, though being an incoherent process in free space, manifests the vacuum Rabi split spectrum characteristic of the strong collective coupling of the atoms to the ‘z’ polarized cavity mode.

III. DISCUSSION

As evidenced above, an important conclusion is that radiation from atomic arrays is not only efficiently collected but is substantially *modified* by the presence of a high-finesse resonator. Most importantly, the strong

coupling to selected resonator modes imposes a *collective* scattering from the atoms into the resonator. This collective coupling, as we have shown, is due to more than simply an interference effect, even in the extremely low intensity limit.

Such coupling can be seen in the vacuum-induced spectral features of our experiment and this points to the possibility that new variants of the Dicke model [57] extended to disordered manifolds with cavity-mediated interactions can be realized and simulated in systems like ours. In fact, considering that multiply excited subradiant states are said to be composed of the superposition of singly excited states in random ensembles [11], our system could be used to provide further insight into this superposition. In particular, such a system is well suited for time-resolved measurements and so the dynamics of the underlying subradiant states in the single-mode limit are now readily available.

Furthermore, we have shown that optical polarization enters the linear scattering regime. On the one hand, the multiple ground-state level structure of atoms has to be taken into account in a linear polarizability description of atoms, beyond the usual scalar polarizability, which was noted as a subtlety in [13]. On the other hand, the multiple ground states open the scene for entanglement-based, new type of subradiant states predicted recently [58]. More generally, the cavity-enhanced polarization rotation could be the design basis for long-range many-body interactions between atoms mediated by two-mode fields. The cavity field fluctuations reflecting a non-trivial atom-cavity spectrum can be exploited as a useful light source when the mean-field is suppressed. Finally, our configuration is very close to schemes for superradiant lasing [44] and for atomic clocks [25] which we hope to explore with the incommensurate lattice trap.

IV. METHODS

Loading atoms into the cavity An ensemble of cold ^{87}Rb atoms was collected in a magneto-optical trap (MOT). After the MOT cycle, the atoms were cooled by polarization gradient cooling ($\sigma^+ - \sigma^-$ configuration) down to temperatures of 20–50 μK . Subsequently, they are magnetically polarized by optical pumping into the $(F, m_F) = (2, 2)$ hyperfine ground state to allow capture with a magnetic quadrupole trap. The magnetically trapped atomic cloud was then transported into the mode of a high-finesse ($\mathcal{F}/\pi = 1430$) resonator by adiabatically displacing the trap center, and was released there by turning off the magnetic field.

The cavity is $l = 15$ mm long and the mode waist is $w = 127$ μm . A far red detuned (805 nm) laser beam was injected into the cavity, serving two purposes: firstly, utilizing the Pound-Drever-Hall technique, the cavity was locked to it, secondly, it provided a far-red-detuned optical dipole lattice for the atoms.

Upon the arrival and release of the atoms, a second

optical pumping was performed into the $(F, m_F) = (2, 2)$ hyperfine ground state defined by a homogeneous magnetic field along ‘z’. The atom number was varied by applying a delay (in the range 8–12 ms, which is safely after the decay of magnetic field transients) before the illumination of the atoms was switched on.

Transverse drive This laser was phase-locked to a reference laser with a variable detuning from the atomic resonance, which we scanned in the frequency range ± 30 MHz. The beam waist was 1 mm, the power in each direction was adjusted from 0.15 μ W to 256 μ W by means of an acousto-optic modulator (AOM). Simultaneously, the $F = 1 \leftrightarrow 2$ transition was also driven resonantly by a repumper laser, in order to keep the atoms in the $F = 2 \leftrightarrow 3$ cycle. The beam waist of the repumper was 12 mm, the power in each direction was 4 mW.

Detection The 805 nm component was removed by interference filters from the cavity output beam which was then split by a polarizing beam splitter. Both the horizontal and vertical polarization beams were coupled into a fibre, connected to a superconducting nanowire single-photon detector (for the measurements shown in Fig. 2) or to a single photon counter module (for the measurements shown in Fig. 3 and Fig. 4). The overall detection efficiency was 7% and 50%, respectively. We recorded few millisecond long signals with time resolution 1 μ s.

Shot-to-shot noise in the atom number In the experiment the averaging over many realizations may involve a random variation of the atom number. On taking this into account, the Eq. (3) is modified and the peak intensity scaling on resonance gets a correction:

$$S_{\max}(\Delta_{\text{peak}}) = \frac{4\eta^2 N^{\beta-1}}{(\kappa + \gamma)^2} \left(1 - \frac{4g^2}{(\kappa + \gamma)^2} \frac{\delta N^2}{\bar{N}} \right), \quad (4)$$

where δN is the variance around the mean \bar{N} . The correction is, however, small for the sub-Poissonian atom number statistics in our MOT.

AUTHOR CONTRIBUTIONS

B.G., K.V.A., and D.N. performed the data acquisition, B.G., B.S., D.N, and P.D. contributed to the data analysis, all authors contributed to the overall operations of the experiment, discussed the results, and worked together on the manuscript.

ACKNOWLEDGEMENTS

This research was supported by the Ministry of Culture and Innovation and the National Research, Development and Innovation Office within the Quantum Information National Laboratory of Hungary (Grant No. 2022-2.1.1-NL-2022-00004), and within the ERANET CO-FUND QuantERA program (MOCA, 2019-2.1.7-ERANET-2022-00041). A. D. acknowledges support from the János Bolyai research scholarship of the Hungarian Academy of Sciences. B. G. acknowledges the support from the ÚNKP-23-3 New National Excellence Program of the Ministry for Culture and Innovation.

-
- [1] M. Gross and S. Haroche. Superradiance: An essay on the theory of collective spontaneous emission. *Physics Reports*, 93(5):301–396, December 1982.
 - [2] R. G. DeVoe and R. G. Brewer. Observation of Superradiant and Subradiant Spontaneous Emission of Two Trapped Ions. *Physical Review Letters*, 76(12):2049–2052, March 1996.
 - [3] S. Inouye, A. P. Chikkatur, D. M. Stamper-Kurn, J. Stenger, D. E. Pritchard, and W. Ketterle. Superradiant Rayleigh Scattering from a Bose-Einstein Condensate. *Science*, 285:571–574, July 1999.
 - [4] Michelle O. Araújo, Ivor Krešić, Robin Kaiser, and William Guerin. Superradiance in a Large and Dilute Cloud of Cold Atoms in the Linear-Optics Regime. *Physical Review Letters*, 117(7):073002, August 2016.
 - [5] Giovanni Ferioli, Antoine Glicenstein, Igor Ferrier-Barbut, and Antoine Browaeys. A non-equilibrium superradiant phase transition in free space. *Nature Physics*, 19(9):1345–1349, September 2023.
 - [6] William Guerin, Michelle O. Araújo, and Robin Kaiser. Subradiance in a Large Cloud of Cold Atoms. *Physical Review Letters*, 116(8):083601, February 2016.
 - [7] Diptaranjan Das, B. Lemberger, and D. D. Yavuz. Subradiance and superradiance-to-subradiance transition in dilute atomic clouds. *Physical Review A*, 102(4):043708, October 2020.
 - [8] Jun Rui, David Wei, Antonio Rubio-Abadal, Simon Hofferlith, Johannes Zeiher, Dan M. Stamper-Kurn, Christian Gross, and Immanuel Bloch. A subradiant optical mirror formed by a single structured atomic layer. *Nature*, 583(7816):369–374, July 2020.
 - [9] D. Plankensteiner, L. Ostermann, H. Ritsch, and C. Genes. Selective protected state preparation of coupled dissipative quantum emitters. *Scientific Reports*, 5(1):16231, November 2015.
 - [10] G. Facchinetti, S. D. Jenkins, and J. Ruostekoski. Storing Light with Subradiant Correlations in Arrays of Atoms. *Physical Review Letters*, 117(24):243601, December 2016.
 - [11] Giovanni Ferioli, Antoine Glicenstein, Loïc Henriët, Igor Ferrier-Barbut, and Antoine Browaeys. Storage and Release of Subradiant Excitations in a Dense Atomic Cloud. *Physical Review X*, 11(2):021031, May 2021.
 - [12] Hashem Zoubi and Helmut Ritsch. Excitons and Cavity Polaritons for Optical Lattice Ultracold Atoms. In *Ad-*

- vances In Atomic, Molecular, and Optical Physics*, volume 62, pages 171–229. Elsevier, 2013.
- [13] A. Asenjo-Garcia, M. Moreno-Cardoner, A. Albrecht, H. J. Kimble, and D. E. Chang. Exponential Improvement in Photon Storage Fidelities Using Subradiance and “Selective Radiance” in Atomic Arrays. *Physical Review X*, 7(3):031024, August 2017.
- [14] P. Solano, P. Barberis-Blostein, F. K. Fatemi, L. A. Orozco, and S. L. Rolston. Super-radiance reveals infinite-range dipole interactions through a nanofiber. *Nature Communications*, 8(1):1857, November 2017.
- [15] Andreas Albrecht, Loïc Henriët, Ana Asenjo-Garcia, Paul B Dieterle, Oskar Painter, and Darrick E Chang. Subradiant states of quantum bits coupled to a one-dimensional waveguide. *New Journal of Physics*, 21(2):025003, February 2019.
- [16] Arjan F. van Loo, Arkady Fedorov, Kevin Lalumière, Barry C. Sanders, Alexandre Blais, and Andreas Wallraff. Photon-Mediated Interactions Between Distant Artificial Atoms. *Science*, 342:1494–1496, 2013. Publisher: American Association for the Advancement of Science.
- [17] René Reimann, Wolfgang Alt, Tobias Kampschulte, Tobias Macha, Lothar Ratschbacher, Natalie Thau, Seokchan Yoon, and Dieter Meschede. Cavity-Modified Collective Rayleigh Scattering of Two Atoms. *Physical Review Letters*, 114(2):023601, January 2015. Publisher: American Physical Society.
- [18] Zhenjie Yan, Jacquelyn Ho, Yue-Hui Lu, Stuart J. Masson, Ana Asenjo-Garcia, and Dan M. Stamper-Kurn. Superradiant and Subradiant Cavity Scattering by Atom Arrays. *Physical Review Letters*, 131(25):253603, December 2023. Publisher: American Physical Society.
- [19] Stefan Nussmann, Markus Hijiikema, Bernhard Weber, Felix Rohde, Gerhard Rempe, and Axel Kuhn. Submicron Positioning of Single Atoms in a Microcavity. *Phys. Rev. Lett.*, 95:173602, October 2005. Publisher: American Physical Society.
- [20] Peter Domokos and Helmut Ritsch. Collective Cooling and Self-Organization of Atoms in a Cavity. *Phys. Rev. Lett.*, 89:253003, 2002. Publisher: American Physical Society.
- [21] Adam T. Black, Hilton W. Chan, and Vladan Vuletić. Observation of Collective Friction Forces due to Spatial Self-Organization of Atoms: From Rayleigh to Bragg Scattering. *Phys. Rev. Lett.*, 91:203001, 2003. Publisher: American Physical Society.
- [22] K. J. Arnold, M. P. Baden, and M. D. Barrett. Self-Organization Threshold Scaling for Thermal Atoms Coupled to a Cavity. *Physical Review Letters*, 109(15):153002, October 2012.
- [23] Sebastian Slama, Gordon Krenz, Simone Bux, Claus Zimmermann, and Philippe W. Courteille. Cavity-enhanced superradiant Rayleigh scattering with ultracold and Bose-Einstein condensed atoms. *Phys. Rev. A*, 75:063620, June 2007. Publisher: American Physical Society.
- [24] Zhiqiang Zhang, Chern Hui Lee, Ravi Kumar, K. J. Arnold, Stuart J. Masson, A. L. Grimsmo, A. S. Parkins, and M. D. Barrett. Dicke-model simulation via cavity-assisted Raman transitions. *Physical Review A*, 97(4):043858, April 2018.
- [25] Eliot A. Bohr, Sofus L. Kristensen, Christoph Hottel, Stefan A. Schäffer, Julian Robinson-Tait, Jan W. Thomsen, Tanya Zelevinsky, Helmut Ritsch, and Jörg H. Müller. Collectively enhanced Ramsey readout by cavity sub- to superradiant transition. *Nature Communications*, 15(1):1084, February 2024. Publisher: Nature Publishing Group.
- [26] Kristian Baumann, Christine Guerlin, Ferdinand Brennecke, and Tilman Esslinger. Dicke quantum phase transition with a superfluid gas in an optical cavity. *Nature*, 464:1301–1306, April 2010. Publisher: Macmillan Publishers Limited. All rights reserved.
- [27] Renate Landig, Lorenz Hruby, Nishant Dogra, Manuele Landini, Rafael Mottl, Tobias Donner, and Tilman Esslinger. Quantum phases from competing short- and long-range interactions in an optical lattice. *Nature*, 532:476–479, April 2016. Publisher: Nature Publishing Group, a division of Macmillan Publishers Limited. All Rights Reserved.
- [28] Julian Léonard, Andrea Morales, Philip Zupancic, Tilman Esslinger, and Tobias Donner. Supersolid formation in a quantum gas breaking a continuous translational symmetry. *Nature*, 543(7643):87–90, March 2017.
- [29] J. Klinder, H. Keßler, M. Reza Bakhtiari, M. Thorwart, and A. Hemmerich. Observation of a Superradiant Mott Insulator in the Dicke-Hubbard Model. *Phys. Rev. Lett.*, 115:230403, 2015. Publisher: American Physical Society.
- [30] Alicia J. Kollár, Alexander T. Papageorge, Varun D. Vaidya, Yudan Guo, Jonathan Keeling, and Benjamin L. Lev. Supermode-density-wave-polariton condensation with a Bose-Einstein condensate in a multimode cavity. *Nature Communications*, 8(1):14386, 2017.
- [31] Juan A. Muniz, Diego Barberena, Robert J. Lewis-Swan, Dylan J. Young, Julia R. K. Cline, Ana Maria Rey, and James K. Thompson. Exploring dynamical phase transitions with cold atoms in an optical cavity. *Nature*, 580(7805):602–607, April 2020.
- [32] Hans Keßler, Phatthamon Kongkhambut, Christoph Georges, Ludwig Mathey, Jayson G. Cosme, and Andreas Hemmerich. Observation of a Dissipative Time Crystal. *Physical Review Letters*, 127(4):043602, July 2021.
- [33] Farokh Mivehvar, Francesco Piazza, Tobias Donner, and Helmut Ritsch. Cavity QED with quantum gases: new paradigms in many-body physics. *Advances in Physics*, 70(1):1–153, January 2021.
- [34] T. W. Clark, A. Dombi, F. I. B. Williams, Á. Kurkó, J. Fortágh, D. Nagy, A. Vukics, and P. Domokos. Time-resolved observation of a dynamical phase transition with atoms in a cavity. *Phys. Rev. A*, 105:063712, Jun 2022.
- [35] B. Gábor, D. Nagy, A. Dombi, T. W. Clark, F. I. B. Williams, K. V. Adwaith, A. Vukics, and P. Domokos. Ground-state bistability of cold atoms in a cavity. *Phys. Rev. A*, 107:023713, Feb 2023.
- [36] Victor Helson, Timo Zwerfner, Farokh Mivehvar, Elvia Colella, Kevin Roux, Hideki Konishi, Helmut Ritsch, and Jean-Philippe Brantut. Density-wave ordering in a unitary Fermi gas with photon-mediated interactions. *Nature*, 618(7966):716–720, June 2023.
- [37] B. Casabone, K. Friebe, B. Brandstätter, K. Schüppert, R. Blatt, and T. E Northup. Enhanced Quantum Interface with Collective Ion-Cavity Coupling. *Physical Review Letters*, 114(2):023602, January 2015.
- [38] A. Neuzner, M. Körber, O. Morin, S. Ritter, and G. Rempe. Interference and dynamics of light from a distance-controlled atom pair in an optical cavity. *Nature Photonics*, 10(5):303–306, May 2016.

- [39] Christoph Hotter, Laurin Ostermann, and Helmut Ritsch. Cavity sub- and superradiance for transversely driven atomic ensembles. *Physical Review Research*, 5(1):013056, January 2023. Publisher: American Physical Society.
- [40] Igor B. Mekhov and Helmut Ritsch. Quantum Nondemolition Measurements and State Preparation in Quantum Gases by Light Detection. *Phys. Rev. Lett.*, 102:020403, 2009. Publisher: American Physical Society.
- [41] William Guerin, Franck Michaud, and Robin Kaiser. Mechanisms for Lasing with Cold Atoms as the Gain Medium. *Physical Review Letters*, 101(9):093002, August 2008.
- [42] Rahul Sawant and S. A. Rangwala. Lasing by driven atoms-cavity system in collective strong coupling regime. *Scientific Reports*, 7(1):11432, September 2017. Publisher: Nature Publishing Group.
- [43] D. Meiser and M. J. Holland. Steady-state superradiance with alkaline-earth-metal atoms. *Physical Review A*, 81(3):033847, March 2010.
- [44] Justin G. Bohnet, Zilong Chen, Joshua M. Weiner, Dominic Meiser, Murray J. Holland, and James K. Thompson. A steady-state superradiant laser with less than one intracavity photon. *Nature*, 484(7392):78–81, April 2012.
- [45] Matthew A. Norcia, Matthew N. Winchester, Julia R. K. Cline, and James K. Thompson. Superradiance on the millihertz linewidth strontium clock transition. *Science Advances*, 2(10):e1601231, October 2016.
- [46] R. J. Thompson, G. Rempe, and H. J. Kimble. Observation of normal-mode splitting for an atom in an optical cavity. *Phys. Rev. Lett.*, 68:1132–1135, 1992. Publisher: American Physical Society.
- [47] A. K. Tuchman, R. Long, G. Vrijsen, J. Boudet, J. Lee, and M. A. Kasevich. Normal-mode splitting with large collective cooperativity. *Physical Review A*, 74(5):053821, November 2006.
- [48] Gessler Hernandez, Jiepeng Zhang, and Yifu Zhu. Vacuum Rabi splitting and intracavity dark state in a cavity-atom system. *Physical Review A*, 76(5):053814, November 2007. Publisher: American Physical Society.
- [49] Geert Vrijsen, Onur Hosten, Jongmin Lee, Simon Bernon, and Mark A. Kasevich. Raman Lasing with a Cold Atom Gain Medium in a High-Finesse Optical Cavity. *Physical Review Letters*, 107(6):063904, August 2011. Publisher: American Physical Society.
- [50] Elmer Suarez, Federico Carollo, Igor Lesanovsky, Beatriz Olmos, Philippe W. Courteille, and Sebastian Slama. Collective atom-cavity coupling and nonlinear dynamics with atoms with multilevel ground states. *Physical Review A*, 107(2):023714, February 2023.
- [51] D. Varga, B. Gábor, B. Sárközi, K.V. Adwaith, D. Nagy, A. Dombi, T.W. Clark, F.I.B. Williams, P. Domokos, and A. Vukics. Loading atoms from a large magnetic trap to a small intra-cavity optical lattice. *Physics Letters A*, 505:129444, 2024.
- [52] Stefano Zippilli, Giovanna Morigi, and Helmut Ritsch. Suppression of Bragg Scattering by Collective Interference of Spatially Ordered Atoms with a High-Q Cavity Mode. *Physical Review Letters*, 93(12):123002, September 2004. Publisher: American Physical Society.
- [53] Haruka Tanji-Suzuki, Ian D. Leroux, Monika H. Schleier-Smith, Marko Cetina, Andrew T. Grier, Jonathan Simon, and Vladan Vuletic. *Interaction between Atomic Ensembles and Optical Resonators: Classical Description*. 2011.
- [54] Helmut Ritsch, Peter Domokos, Ferdinand Brennecke, and Tilman Esslinger. Cold atoms in cavity-generated dynamical optical potentials. *Rev. Mod. Phys.*, 85:553–601, April 2013. Publisher: American Physical Society.
- [55] Tatjana Wilk, Simon C. Webster, Axel Kuhn, and Gerhard Rempe. Single-Atom Single-Photon Quantum Interface. *Science*, 317(5837):488–490, July 2007.
- [56] Holger P. Specht, Christian Nölleke, Andreas Reiserer, Manuel Uphoff, Eden Figueroa, Stephan Ritter, and Gerhard Rempe. A single-atom quantum memory. *Nature*, 473(7346):190–193, May 2011.
- [57] Zhang Zhiqiang, Chern Hui Lee, Ravi Kumar, K. J. Arnold, Stuart J. Masson, A. S. Parkins, and M. D. Barrett. Nonequilibrium phase transition in a spin-1 Dicke model. *Optica*, 4(4):424, April 2017.
- [58] Martin Hebenstreit, Barbara Kraus, Laurin Ostermann, and Helmut Ritsch. Subradiance via Entanglement in Atoms with Several Independent Decay Channels. *Physical Review Letters*, 118(14):143602, April 2017.